CRYSTAL GROWTH & DESIGN

pubs.acs.org/crystal

Article

Control of Regioselectivity in the Dimerization of *trans*-Cinnamic Acid and Its Derivatives Using Cocrystal Engineering

Carole Body, Guillaume Wery, Lisa Gubbels, Koen Robeyns, and Tom Leyssens*

Cite This: *Cryst. Growth Des.* 2024, 24, 2117−2125

Read Online

ACCESS | Metrics & More | Article Recommendations | Supporting Information

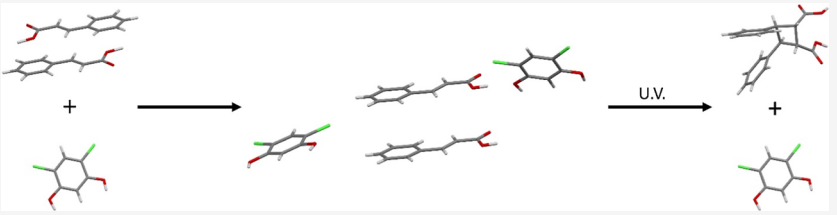

ABSTRACT: *trans*-Cinnamic acid and derivatives can undergo a [2 + 2] photocycloaddition, resulting in the formation of truxinic and truxillic acids. These photoproducts are regioisomers, differing only in the relative arrangement of the acid and phenyl groups on the cyclobutane ring formed. In this contribution, we show that a cocrystal engineering approach can direct the outcome of the reaction (regioisomer) and control the photoreactivity of the compounds in the solid state. For *trans*-cinnamic acid, cocrystallization with 4,6-dichlororesorcinol yields a thermodynamic pathway to *β*-truxinic acid. The otherwise photostable *para*-methoxy-*trans*-cinnamic acid can be rendered photoactive to also yield *β*-truxinic acid using 5-hydroxyisophthalic acid. Finally, the photoactive *para*-hydroxy-*trans*cinnamic acid can be rendered photostable by cocrystallization. Cocrystal engineering is thus a valuable tool not only to control photoreactivity but also the obtained outcome of a solid-state photoreaction. We expect to see this approach being applied as a more general procedure for this type of reaction in the future.

1. INTRODUCTION

A [2 + 2] photocycloaddition leads to the formation of a cyclobutane derivative, converting two *π*-bonds into two *σ*-bonds upon irradiation.[1] Conducting this reaction in the solid state eliminates the need for solvents, aligning with one of the 12 principles of green chemistry aimed at promoting more sustainable chemical practices to address contemporary environmental challenges.[2]

From 1964 onward, Cohen and Schmidt extensively investigated these reactions and observed that the resulting products correlate with the initial crystal lattice structure. This topochemical relationship is based on different observations:

1. Differences in behavior upon irradiation of different polymorphs.
2. Fundamental differences in photoproducts between two derivatives of a given compound.
3. Differences in solid-state reactivity compared to reactivity in solution.

These observations led to the postulation that "reaction in the solid state occurs with a minimum amount of atomic or molecular movement".[3,4] This further underscores the advantage of solid-state reactions, allowing for the attainment of regioselective and stereospecific products, which are often challenging to achieve in solution-phase reactions.[5] Later, Schmidt established two fundamental conditions necessary for cycloadditions to occur in the solid state: the double bonds must be parallel, and the distance between them should be shorter than 4.2 Å.[6]

trans-Cinnamic acid (TCA) and its derivatives nicely illustrate these principles. Within this chemical family, solid forms can be categorized into three types:

- The *α*-type, photoreactive and characterized by a "head-to-tail" (HTT) packing arrangement.
- The *β*-type, photoreactive and characterized by a "head-to-head" (HTH) packing arrangement.
- The *γ*-type being photostable.[7,8]

One should note that not all derivatives exhibit all three types. For example, TCA lacks a *γ*-type form, having only one *α*- and one *β*-type form.[9] The *α*-type (also called *α*-polymorph) is the stable form, whereas the *β*-type (*β*-polymorph) is metastable, transforming into the *α*-polymorph over time. Furthermore, both forms lead to a different product upon irradiation: *α*-truxillic acid is obtained by irradiating the *α*-form, whereas the *β*-form leads to *β*-truxinic acid, although experimentally a mixture of *α*-truxillic acid and *β*-truxinic acids

Received: December 5, 2023
Revised: January 29, 2024
Accepted: January 30, 2024
Published: February 21, 2024

https://doi.org/10.1021/acs.cgd.3c01449
Cryst. Growth Des. 2024, 24, 2117−2125

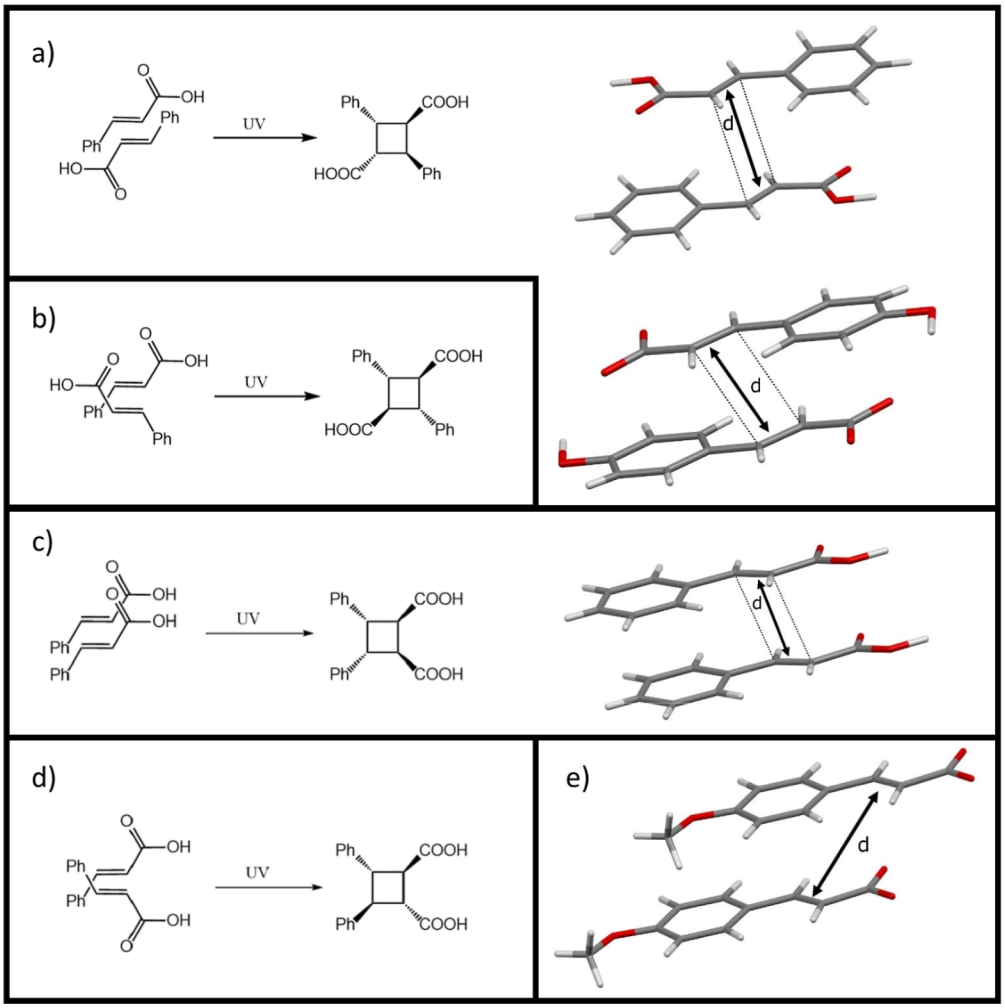

Figure 1. (a) α-Type (HTT orientation). Scheme representing the photoreactivity of TCA in the α-type, the crystal structure of the α-polymorph of TCA[12] (top, d = 3.7 Å), and this of *p*-OH-TCA[13] (bottom, d = 3.8 Å); (b) ε-type (HTT orientation). Scheme representing the photoreactivity of TCA in the theoretical ε-type; (c) β-type (HTH orientation). Scheme representing the photoreactivity of TCA in the β-type and the crystal structure of the β-polymorph of TCA[14] (d = 4.0 Å); (d) δ-type (HTH orientation). Scheme representing the photoreactivity of TCA in the theoretical δ-type; (e) γ-type (no reaction). Crystal structure of *p*-OMe-TCA[12] (d = 4.8 Å). The dotted lines represent the bonds formed after irradiation.

is observed due to the metastable character of the β-polymorph (Figure 1a,c).[8] In solution, TCA remains photostable.[3] The behavior of other derivatives can vary significantly; for instance, *para*-hydroxy-TCA (*p*-OH-TCA), *ortho*-chloro-TCA, and *para*-methoxy-TCA (*p*-OMe-TCA) have only one known polymorph, respectively, of the α-, β-, and γ-type (Figure 1a,e), explaining the different outcome for these compounds upon irradiation.[9]

Besides α-truxillic and β-truxinic acids, two other products are theoretically accessible by photodimerization of TCA: δ-truxinic[10] and ε-truxillic acids.[11] These products are accessible through structural types other than those described above. In this work, these packages are, respectively, named the δ- and the ε-type (Figure 1b,d).

In 2010, Desiraju defined crystal engineering as "the understanding of intermolecular interactions in the context of crystal packing and in the utilization of such understanding in the design of new solids with desired physical and chemical properties".[15] We here apply this concept to control the [2 + 2] photocycloaddition by forming cocrystals, which in the context of this work are considered as a multicomponent solid form consisting of neutral molecules that are not a solvent known as coformers.[16] Some examples are already shown in the literature where cocrystallization has been used to render photostable compounds photoactive. Resorcinol and its derivatives are a common family used to orient the target molecules to meet Schmidt's criteria.[17] MacGillivray et al. successfully dimerized *trans*-1,2-bis(4-pyridyl)ethylene by cocrystallization with resorcinol.[18] Friščić et al. constructed *exo,exo*[2,2]orthocyclophane and *exo,exo*[2,2]metacyclophane using 4-chloro-resorcinol while *endo,exo*[2,2]metacyclophane is obtained using 4-cyclohexyl-resorcinol.[19] [*n*]Ladderanes (*n* = 3, 5, 7) are also synthesized in the solid state from all-trans-poly *m*-enes (*m* = 2, 3, 4) through cocrystallization with resorcinol.[20−22]

For dimerizing molecules containing carboxylic acids,[23] pyridyl can replace resorcinol to orient the compounds through the formation of H-bonds.[24,25] In their review, Akhtaruzzaman et al.[17] explained that other molecules, such as carboxylic acids, boronic acid,[26] and thiourea, can serve as templates for solid-state dimerization.

https://doi.org/10.1021/acs.cgd.3c01449
Cryst. Growth Des. 2024, 24, 2117−2125

Scheme 1. Approach Used: The Stable Form of TCA Is of the α-Type[a]

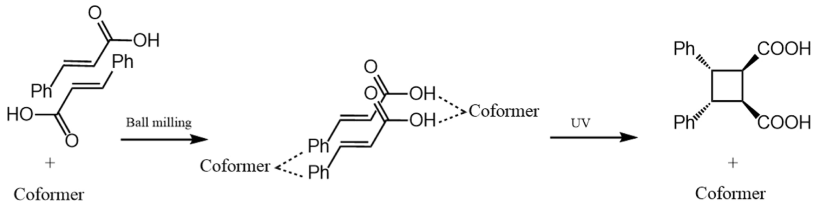

[a]By cocrystallization, a stable form of the β-type can be achieved, offering a thermodynamically stable pathway to β-truxinic acid.

In addition to these hydrogen-bonded systems, alternative interactions have been used to align olefins for dimerization, such as, halogen bonding systems,[27−31] boron compounds used as Lewis acid,[32,33] host−guest system with cucurbit[8]uril used as host,[34] and anion stacking.[35]

As mentioned above, the β-polymorph of TCA (crystallizing in the β-type) is metastable, with its irradiation leading to a mixture of β-truxinic and α-truxillic acids. Several strategies have been put forward to come to a stable β-type structure of TCA. Ito et al. controlled the dimerization by forming diamine salt forms to obtain β-truxinic or ε-truxillic acids after irradiation.[36] In a different approach, a covalent bond can be created between the acid and various templates, such as 1,8-dihydroxynaphthalene or diamino[2.2]paracyclophane, leading to β-truxinic acid after irradiation either in solution or in the solid state.[37−40] However, this method requires an additional hydrolysis step to remove the template. In most of the above examples, molecules undergoing solid-state dimerization via cocrystallization are highly symmetric, with the alkene compound containing two carboxylic acid groups or two heteroaromatic cycles.

In this paper, we set out to complement these studies, aiming for cocrystals with TCA and some of its derivatives (*p*-OH-TCA and *p*-OMe-TCA) with the goal of synthesizing photoproducts different from those obtained using the stable form of the parent compound. All three compounds are highly asymmetric with different functional groups substituting the double bond (e.g., −COOH and −Ph groups for the TCA molecule), showing the viability of this approach even for those compounds which are not highly symmetrical (Scheme 1).

2. EXPERIMENTAL SECTION

2.1. Materials. All solvents used are commercially available from VWR. Solvents were used as received without any additional purification. *trans*-Cinnamic acid (TCA) (97%), urea (99%), 3,4-dihydroxybenzoic acid (97%), and 3-nitrobenzoic acid (99%) were obtained from Sigma-Aldrich. The two derivatives, *p*-OMe-TCA (98%) and *p*-OH-TCA (98%), as well as 4,6-dichlororesorcinol (96%) were purchased from TCI. 4,4′-Bipyridine (98%), 4-amino-benzoic acid (99%), and 5-hydroxyisophthalic acid (98%) were furnished by Alfa Aesar, and 4-nitrobenzoic acid (>99%) was purchased from Acros. All these products were used as received.

2.2. Methods. *2.2.1. Cocrystal Screening.* Cocrystal screening was performed by liquid-assisted grinding (LAG), using a Retsch Mixer Mill MM 400 equipped with two grinding jars each able to contain five 2 mL Eppendorf tubes. Each tube was filled with equimolar amounts (0.1 mmol) of a TCA derivative and coformer, three small stainless-steel beads (3 mm of diameter), and 10 μL of methanol. Grinding was then performed at 30 Hz for 90 min.

2.2.2. Single-Crystal Growth. Single-crystal growth was achieved through evaporative crystallization, performed by preparing under-saturated solutions of equimolar amounts of the 2 molecules forming the cocrystal in a suitable amount of solvent. The solutions were then left to evaporate slowly, either at room temperature or in the fridge (5 °C), and the crystals were retrieved once they appeared.

2.2.3. Powder X-ray Diffraction (XRPD). Powder X-ray diffraction data were collected on a PANalytical Bragg−Brentano diffractometer, using Ni-filtered Cu Kα (λ = 1.54179 Å) at 45 kV and 30 mA with a X'Celerator detector. Each sample was analyzed between 5 and 35° in 2θ with a step size of ca. 0.02° and a total scan time of 50 min.

2.2.4. Single-Crystal X-ray Diffraction (SCXRD). Single-crystal X-ray diffraction was performed on a suitable single crystal and analyzed on a MAR345 image plate using Mo Kα radiation generated by an Incoatec IμS microfocus source (Montel mirrors). Data reduction was carried out using the CrysAlisPRO software package.[41] The resolution and refinement by full-matrix least-squares were carried out using, respectively, SHELXT[42] and SHELX-2018/3.[43] Non-hydrogen atoms were refined anisotropically; H atoms were added in calculated positions and allowed to ride on the parent atoms, with isotropic displacement factors set to 1.2 equiv of the parent atoms [U_{iso}(H) = 1.5U_{eq}(C) for methyl en OH hydrogens]. The H atoms of the methyl groups were allowed to undergo free rotation about the local 3-fold axis. Symmetry analysis and validation were carried out using PLATON.[44] Figures were drawn using the molecular visualization software Mercury 2022.3.0.[45]

2.2.5. Irradiation. The cocrystal powder was placed between two glass plates, which were then sealed together. The compound was photoactivated with a UV lamp, specifically the "Oriel Instrument: Universal Arc Lamp Housing" [model: 66921; source: Hg(Xe)], at 350 W for 48 h. It was turned over every hour to have an equivalent irradiation time for each side. The irradiation products obtained are examined through ^{1}H NMR spectroscopy, employing a Bruker-300 spectrometer operating at 300 MHz. The NMR spectra were captured in DMSO-d_6, internally referenced to residual solvent (^{1}H) resonances, and expressed relative to tetramethylsilane. Chemical shifts are reported in ppm with tetramethylsilane as the reference.

3. RESULTS AND DISCUSSION

3.1. Cocrystal Discovery. As a first step, we identified novel cocrystal forms of the three target compounds. This was done through MeOH-based LAG using common cocrystal coformers, typically reacting with carboxylic acids. Seven new crystalline forms were identified for TCA, 6 for *p*-OMe-TCA, and 2 for *p*-OH-TCA. Table 1 provides a summary of the cocrystals formed through grinding, and Figure 2 shows the coformers used. The XRPD overlays are given in the Supporting Information (Figures S1−S15).

3.2. Solid-State Reactivity of the Novel Cocrystals. The photobehavior of the newly formed cocrystals was analyzed experimentally, verifying the product outcome using ^{1}H NMR spectroscopy. If, following irradiation, only the starting material is detected, then no reaction occurred. Conversely, the presence of supplementary peaks around δ = 4 ppm suggests dimerization. Figure 3 shows an example of the ^{1}H NMR spectra of a photoactive cocrystal. (As the photochemical reaction occurs on the surface of the crystals, only partial transformation occurs so a mixture of starting materials and reacted material is visible in the 1H NMR. This

https://doi.org/10.1021/acs.cgd.3c01449
Cryst. Growth Des. 2024, 24, 2117−2125

Table 1. New Cocrystal Forms of TCA, *p*-OMe-TCA, and *p*-OH-TCA[a]

	TCA	p-OMe-TCA	p-OH-TCA
3,4-dihydroxybenzoic acid	+	+	
3-nitrobenzoic acid	+	+	
4,4'-bipyridine	+	+	+
4,6-dichlororesorcinol	+		
4-aminobenzoic acid	+	+	
4-nitrobenzoic acid	+	+	
5-hydroxyisophtalic acid		+	
Urea	+		+

[a]+ = new crystalline form identified during the grinding experiment, dark gray = no new crystalline form identified.

partial transformation could be avoided by changing the experimental setup (e.g., irradiation under mixing).) All other spectra are available in the Supporting Information (Figures S16−S29). Distinguishing between α-truxillic acid and β-truxinic acid can be done by looking at the signal's multiplicity, as depicted in Figure 4. In parallel, we aimed at obtaining the crystal structures to see whether they indeed confirm the observed outcome. Table 2 provides a summary of the various cocrystals identified, each of which will be further developed in subsequent sections. From a first look at this table, different tendencies can be drawn. Ignoring the three cocrystals for which no structure has yet been obtained, the photoproduct corresponds perfectly with the outcome expected from the crystal structure. Table 2 also shows that cocrystallization can render photostable products photoactive, e.g., *p*-OMe-TCA is photostable, but its cocrystal with 5-hydroxyisophthalic acid leads to a β-product, or photoactive compounds photostable, e.g., TCA is photoreactive, but its cocrystal with 3-nitrobenzoic acid is photostable. Finally and importantly, cocrystallization can successfully be used to thermodynamically control the nature of the photoproduct. TCA can be transformed in pure β-truxinic acid in a controlled manner using 4,6-dichlororesorcinol as a coformer, in α-truxillic acid using 3,4-dihydroxybenzoic acid, and rendered photostable using urea. Similar observations can be made for *p*-OMe-TCA or *p*-OH-TCA even if for these no coformer leading to, respectively, the α- and β-products has yet been identified.

3.2.1. trans-Cinnamic Acid. As mentioned, the stable polymorph of TCA packs into the α-type. Identifying a stable solid form of the β-, δ-, or ε-type is of interest, as this would offer a thermodynamic pathway to, respectively, β-truxinic, δ-truxinic, or ε-truxillic acids.

Seven coformers led to cocrystal formation, all of which are structurally described here. As 2 polymorphs are obtained for the cocrystal with 4,4′-bipyridine, a total of 8 cocrystal phases were identified for this compound. Table 2 shows that cocrystallization in most cases deactivates the photoreactive behavior of TCA. 6 out of the 8 solid forms are not reactive. The use of 3,4-dihydroxybenzoic acid as a coformer leads to α-truxillic acid. Interestingly, the use of 4,6-dichlororesorcinol leads to β-truxinic acid only. The 4,6-dichlororesorcinol cocrystal is therefore a thermodynamically stable form, which can yield access to β-truxinic acid, where the metastable β-polymorph of TCA results in a mixture of β-truxinic and α-truxillic acid.

To get a deeper understanding of TCA cocrystal reactivity, Table 3 summarizes the main structural elements. A selected number of structures are described below, with all others shown in the Supporting Information (Figures S30−S43).

Table 3 confirms that the addition of a coformer most often renders the cocrystal photostable. This can either occur due to the intercalation of the coformer between TCA molecules, as is the case for 3-nitrobenzoic (Figure 5) and 4-nitrobenzoic acid cocrystals, or due to the elongated distance between two TCA molecules, as it is the case for 4,4′-bipyridine (polymorphs I and II), 4-aminobenzoic acid, and urea.

The cocrystal involving 3,4-dihydroxybenzoic acid (Figure 6) shows structural features (direct contact between two TCA molecules, parallel C═C bonds separated by 3.8 Å), which, combined with a head-to-tail packing, successfully lead to the formation of α-truxinic acid.

A similar observation can be made for the 4,6-dichlororesorcinol-TCA cocrystal (Figure 7) where favorable structural features (direct contact between TCA molecules, parallel C═C bonds separated by 3.9 Å) combined with a head-to-head orientation explain the formation of β-truxillic acid upon irradiation. Interestingly, as stated above, this isomer cannot be obtained in pure form starting from the metastable β-polymorph of TCA, as this later readily transforms into the α-polymorph. We thus present a thermodynamic pathway to β-truxillic acid using a cocrystallization tool. On top of that, after reactivity, 4,6-dichlororesorcinol could potentially be recovered from the resulting powder and reused if needed. This can, e.g., be done by slurrying the final powder in a solvent, such as

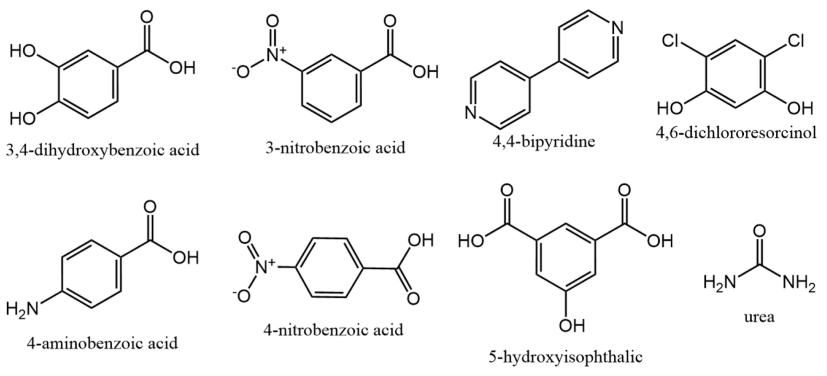

Figure 2. Representation of the molecules forming cocrystals with TCA, *p*-OMe-TCA, and *p*-OH-TCA.

https://doi.org/10.1021/acs.cgd.3c01449
Cryst. Growth Des. 2024, 24, 2117−2125

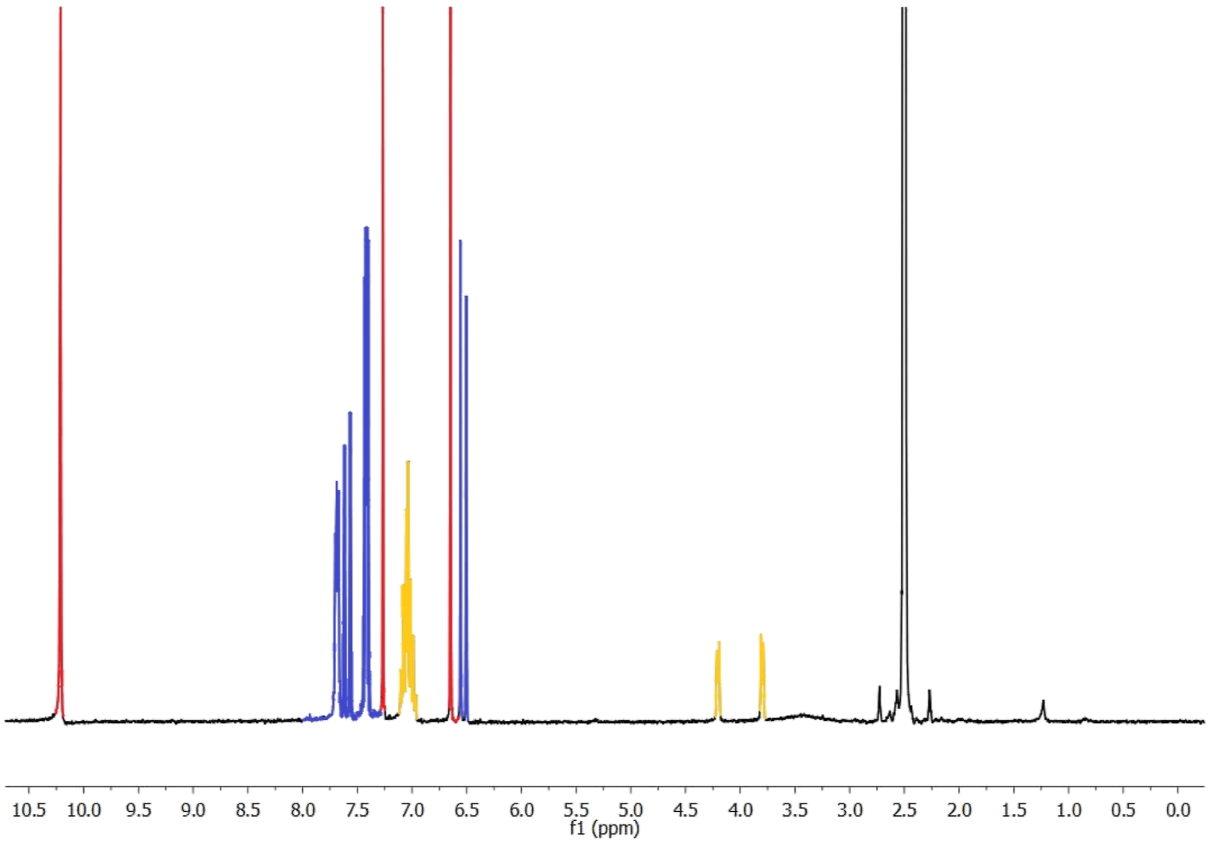

Figure 3. ^{1}H NMR spectrum of the irradiated cocrystal constituted of TCA and 4,6-dichlororesorcinol (red peaks: 4,6-dichlororesorcinol; blue peaks: TCA; yellow peaks: α-truxillic acid).

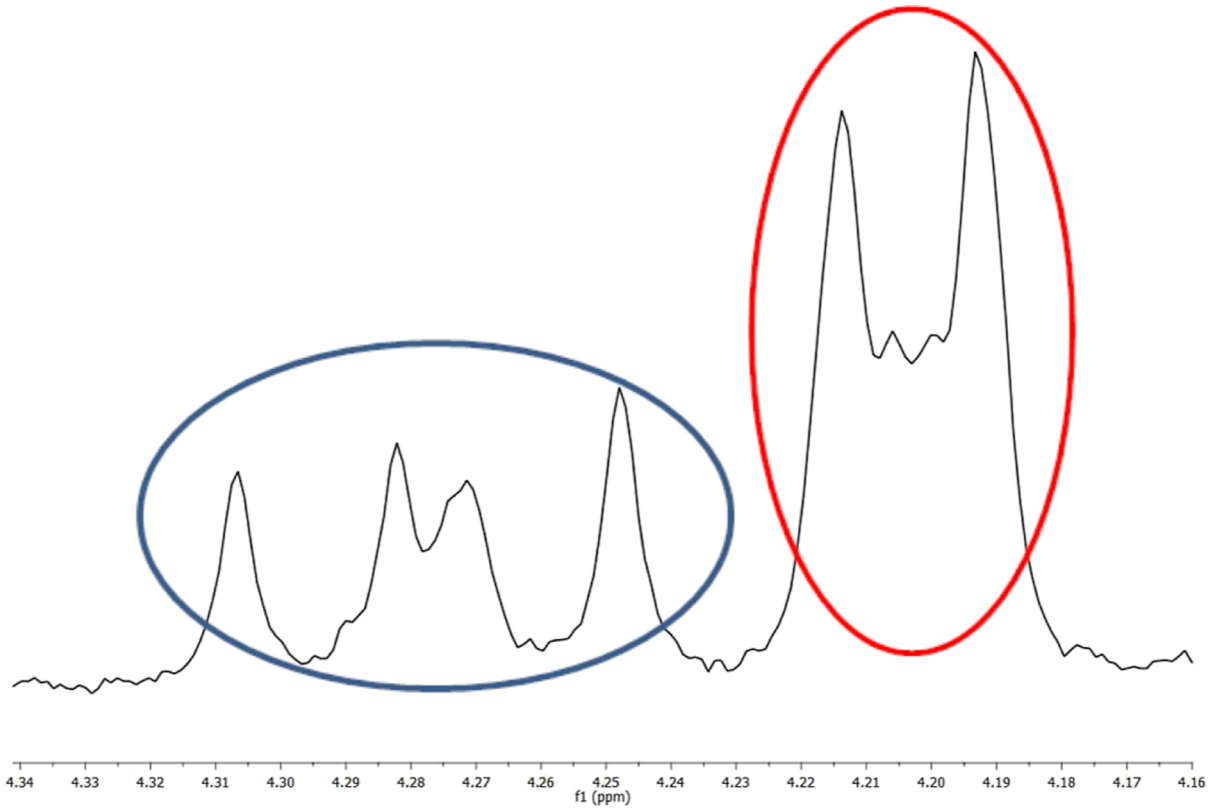

Figure 4. Characteristic peaks of α-truxillic acid (blue) and β-truxinic acid (red) obtained by the irradiation of a sample of a mixture of TCA β and α-polymorphs.

https://doi.org/10.1021/acs.cgd.3c01449
Cryst. Growth Des. 2024, 24, 2117−2125

Table 2. Outcome upon Irradiation as Well as Expected Outcome Based on the Crystal Structure of Various Cocrystals[a]

Coformer	TCA		p-OMe-TCA		p-OH-TCA	
	Irr.	Cryst.	Irr.	Cryst.	Irr.	Cryst.
/	α-product	α-type[b]	No Reaction	γ-type[c]	α-product	α-type[d]
3,4-dihydroxybenzoic acid	α-product	α-type				
3-nitrobenzoic acid	No Reaction	γ-type	No Reaction	γ-type		
4,4'-bipyridine	I : No Reaction	I : γ-type	No Reaction	γ-type[e]	No Reaction	γ-type
	//	II : γ-type				
4,6-dichlororesorcinol	β-product	β-type				
4-aminobenzoic acid	No Reaction	γ-type	No Reaction	/		
4-nitrobenzoic acid	No Reaction	γ-type	I : No Reaction	I : γ-type		
			//	II : γ-type		
5-hydroxyisophtalic acid			β-product	/		
Urea	No Reaction	γ-type			α-product	α-type

[a]Dark gray box means no cocrystal occurred for this particular combination. / means single crystal structure could not be determined. // means no sufficient bulk powder was obtained to perform reactivity studies. [b]CCDC code: CINMAC.[12] [c]CCDC code: MXCINN.[12] [d]CCDC code: COUMAC01.[13] [e]CCDC code: NUZTOT.[48]

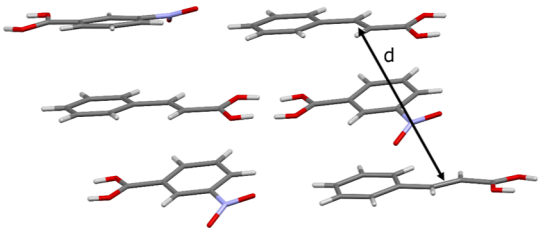

Figure 5. Example of a cocrystal packed in the γ-type. This cocrystal is constituted of TCA and 3-nitrobenzoic acid (d = 7.5 Å).

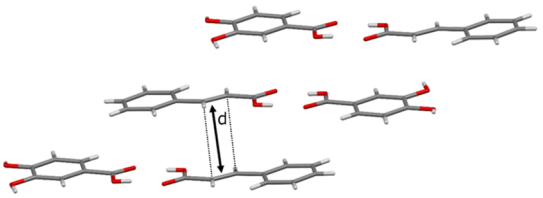

Figure 6. Example of a cocrystal packed in the α-type. This cocrystal is constituted of TCA and 3,4-dihydroxybenzoic acid (d = 3.8 Å).

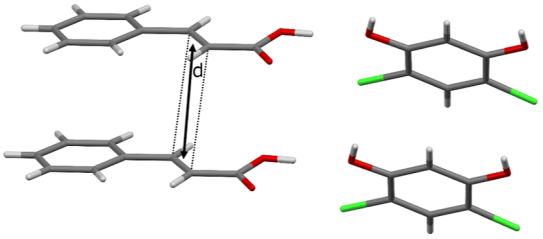

Figure 7. Example of a cocrystal packed in the β-type. This cocrystal is constituted of TCA and 4,6-dichlororesorcinol (d = 3.9 Å).

water, where 4,6-dichlororesorcinol is soluble but TCA and its dimer are not.[46,47]

Table 3 also indicates that achieving HTH or HHT orientations is equally accessible and feasible. However, this does not suffice to obtain the right product, as for reactivity to occur structural features (distance and alignment of double bonds) are key.

3.2.2. para-Methoxy-TCA (p-OMe-TCA) and para-Hydroxy-TCA (p-OH-TCA). Contrary to TCA, *p*-OMe-TCA packs in the γ-type and is hence photoinactive.

Six different cocrystal forms were identified, with 4 structurally described, one of which was already published. Five of these forms are of the γ-type as no reaction occurred. (For those cases where no single crystals were identified, the γ-type was determined based on the nonreactivity observed by 1H NMR.) Table 2 shows that in most cases, cocrystallization does not impact the reactivity of *p*-OMe-TCA, as 5 out of the 6 cases remain unreactive. Only the use of 5-hydroxysophtalic acid as a coformer leads to a photoreactive cocrystal, where the β-product is obtained after irradiation. Table 4 summarizes the features, allowing us to understand the reactivity of the cocrystal.

As shown by Table 4, once more, both HTH and HTT orientations can be obtained, but in most cases, the double bonds are not in sufficient proximity to allow photoreactivity.

Interestingly, the cocrystal of *p*-OMe-TCA with 5-hydroxyisophthalic acid exhibits photoreactivity, leading to the formation of di-4-methoxy-β-truxinic acid. This product

Table 3. Characteristics of the 8 Structurally Identified Cocrystal Forms Discovered with TCA [Intercalation of the Coformer between Two Successive TCA Molecules, Relative Orientation of TCA Molecules in a Head-To-Tail (HTT) or Head-To-Head (HTH) Fashion, Parallel or Non-parallel Orientation of Two Double Bonds, and Distance between the Center of the Double Bonds]

coformer		intercalation	orientation	parallel	distance [Å]	photoproduct
3,4-dihydroxybenzoic acid		no	HTT	yes	3.8	α-product
3-nitrobenzoic acid		yes	HTH	no	7.5	no reaction
4,4′-bipyridine	polymorph I	no	HTT	yes	5.6	no reaction
	polymorph II	no	HTH	no	5.1	no reaction
4,6-dichlororesorcinol		no	HTH	yes	3.9	β-product
4-aminobenzoic acid		no	HTH	yes	4.9	no reaction
4-nitrobenzoic acid		yes	HTH	yes	7.4	no reaction
urea		no	HTT	yes	4.6	no reaction

https://doi.org/10.1021/acs.cgd.3c01449
Cryst. Growth Des. 2024, 24, 2117−2125

Table 4. Characteristic of the Structurally Identified Cocrystals for *p*-OMe-TCA and *p*-OH-TCA (Intercalation of the Coformer between Two Successive TCA Molecules, Relative Orientation of TCA Molecules in a Head-To-Tail or Head-To-Head Fashion, Parallel or Non-parallel Orientation of Two Double Bonds, and Average Distance between the Double Bonds)

coformer		intercalation	orientation	parallel	distance [Å]	photoproduct
			p-OMe-TCA			
3-nitrobenzoic acid		Yes	HTH	yes	7.3	no reaction
4,4′-bipyridine[48]		No	HTH	yes	6.5	no reaction
4-nitrobenzoic acid	polymorph I	No	HTT	yes	5.3	no reaction
	polymorph II	Yes	HTH	yes	7.4	no reaction
			p-OH-TCA			
4,4′-bipyridine		No	HTH	no	7.7	no reaction
urea		No	HTT	yes	3.8	*α*-product

cannot be obtained from the photostable starting material. Based on the photoproduct, we suspect that this cocrystal shows an HTH orientation with parallel aligned double bonds.

As for TCA, *p*-OH-TCA packs in the *α*-type. Two cocrystals were identified for this compound (Table 2). Cocrystallization with urea leads to *α*-type packing, whereas cocrystallization with 4,4′-bipyridine renders the product photostable. Both results are expected based on the crystal structure (Table 4). The photostability of the 4,4′-bipyridine cocrystal is due to the considerable distance between the double bonds. It should be noted that the molecules have an HTH orientation. The urea cocrystal, on the other hand, shows an HTT orientation with a mere 3.8 Å between the double bonds (Figure 8).

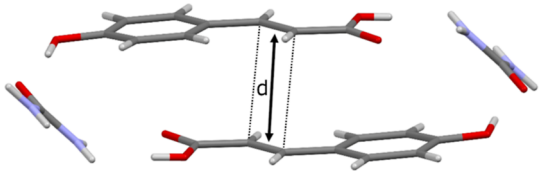

Figure 8. Structural feature of the cocrystal constituted of *p*-OH-TCA and urea (d = 3.8 Å).

4. CONCLUSIONS

In this contribution, we extend the solid-state photodimerization of TCA and two of its derivatives, showing how cocrystallization can be used to engineer the solid state in such a way as to thermodynamically control the regioisomer obtained. Focusing on TCA, *p*-OMe-TCA, and *p*-OH-TCA, we show that both the head-to-head and head-to-tail orientations have a similar likelihood of occurring in the cocrystals but that the alignment of and distance between double bonds is often the limiting factor for photoreactivity. Given an appropriate coformer, however, photoreactivity can be controlled. For TCA, we show that cocrystallization with 4,6-dichlororesorcinol is a thermodynamically stable pathway to *β*-truxinic acid, whereas the stable polymorph of the parent compound yields *α*-truxillic acid. For *p*-OH-Me, the use of 4,4′-bipyridine allows rendering the otherwise photoactive molecule photoinactive. And for *p*-OMe-TCA, *β*-truxinic acid is obtained when orienting the compound with 5-hydroxyisophthalic acid, whereas the parent compound is photoinactive.

This study was performed using a limited series of coformers but shows how cocrystal engineering can effectively be used not only to activate (or deactivate) photoreactivity but also as a pathway to thermodynamically control the regioisomer of the photoproduct obtained.

■ ASSOCIATED CONTENT

Supporting Information

The Supporting Information is available free of charge at https://pubs.acs.org/doi/10.1021/acs.cgd.3c01449.

Grinding results, ^{1}H NMR, representation of the main structural elements of cocrystal structures, solution synthesis of cocrystal material for which no single crystal was obtained, and single crystals (PDF)

Accession Codes

CCDC 2312228−2312240 contain the supplementary crystallographic data for this paper. These data can be obtained free of charge via www.ccdc.cam.ac.uk/data_request/cif, or by emailing data_request@ccdc.cam.ac.uk, or by contacting The Cambridge Crystallographic Data Centre, 12 Union Road, Cambridge CB2 1EZ, UK; fax: +44 1223 336033.

■ AUTHOR INFORMATION

Corresponding Author

Tom Leyssens − *UCLouvain, 1348 Ottignies-Louvain-la-Neuve, Belgium*; orcid.org/0000-0001-7916-1373; Email: tom.leyssens@uclouvain.be

Authors

Carole Body − *UCLouvain, 1348 Ottignies-Louvain-la-Neuve, Belgium*

Guillaume Wery − *UCLouvain, 1348 Ottignies-Louvain-la-Neuve, Belgium*

Lisa Gubbels − *UCLouvain, 1348 Ottignies-Louvain-la-Neuve, Belgium*

Koen Robeyns − *UCLouvain, 1348 Ottignies-Louvain-la-Neuve, Belgium*; orcid.org/0000-0002-4763-4217

Complete contact information is available at: https://pubs.acs.org/10.1021/acs.cgd.3c01449

Notes

The authors declare no competing financial interest.

■ ACKNOWLEDGMENTS

C.B., K.R., and T.L. would like to thank the FNRS for financial support PDR grants (T.0149.19−T.262.20) and CDR J.0168.22. G.W. is UCLouvain scholarship recipient.

■ REFERENCES

(1) Bruice, P. Y. Pericyclic Reactions. In *Organic Chemistry*; Prentice-Hall, 2011; pp 1209−1225.

(2) Jessop, P. G.; Trakhtenberg, S.; Warner, J. The Twelve Principles of Green Chemistry. In *Innovations in Industrial and Engineering Chemistry*; American Chemical Society, 2009; pp 401−436.
(3) Cohen, M. D.; Schmidt, G. M. J. 383. Topochemistry. Part I. A survey. *J. Chem. Soc.* **1964**, 1996−2000.
(4) Cohen, M. D. Solid-State Photochemical Reactions. *Tetrahedron* **1987**, *43* (7), 1211−1224.
(5) Ramamurthy, V.; Sivaguru, J. Supramolecular Photochemistry as a Potential Synthetic Tool: Photocycloaddition. *Chem. Rev.* **2016**, *116* (17), 9914−9993.
(6) Schmidt, G. M. J. Photodimerization in the Solid State. *Pure Appl. Chem.* **1971**, *27* (4), 647−678.
(7) Cohen, M. D.; Schmidt, G. M. J.; Sonntag, F. I. 384. Topochemistry. Part II. The photochemistry of trans-cinnamic acids. *J. Chem. Soc.* **1964**, 2000−2013.
(8) Amjaour, H.; Wang, Z.; Mabin, M.; Puttkammer, J.; Busch, S.; Chu, Q. R. Scalable preparation and property investigation of a *cis*-cyclobutane-1,2-dicarboxylic acid from *β-trans*-cinnamic acid. *Chem. Commun.* **2019**, *55* (2), 214−217.
(9) Schmidt, G. M. J. 385. Topochemistry. Part III. The crystal chemistry of some trans-cinnamic acids. *J. Chem. Soc.* **1964**, 2014−2021.
(10) National Center for Biotechnology Information. *PubChem Compound Summary for CID 25245913*; PubChem, 2022.
(11) National Center for Biotechnology Information. *Substance Record for SID 273537784, 528-38-1, Source: Japan Chemical Substance Dictionary (Nikkaji)*; PubChem. https://pubchem.ncbi.nlm.nih.gov/substance/273537784 (accessed June 09, 2023).
(12) Bryan, R. F.; Freyberg, D. P. Crystal Structures of α-Trans- and p-Methoxy-Cinnamic Acids and Their Relation to Thermal Mesomorphism. *J. Chem. Soc., Perkin Trans. 2* **1975**, *181* (15), 1835−1840.
(13) Bryan, R. F.; Forcier, P. G. Crystal Structure Basis for the Absence of Thermal Mesomorphism in P-Hydroxy- Trans-Cinnamic Acid. *Mol. Cryst. Liq. Cryst.* **1980**, *60* (3), 157−165.
(14) Abdelmoty, I.; Buchholz, V.; Di, L.; Guo, C.; Kowitz, K.; Enkelmann, V.; Wegner, G.; Foxman, B. M. Polymorphism of Cinnamic and α-Truxillic Acids: New Additions to an Old Story. *Cryst. Growth Des.* **2005**, *5* (6), 2210−2217.
(15) Desiraju, G. R. Crystal Engineering: A Brief Overview. *J. Chem. Sci.* **2010**, *122* (5), 667−675.
(16) Grothe, E.; Meekes, H.; Vlieg, E.; Ter Horst, J. H.; De Gelder, R. Solvates, Salts, and Cocrystals: A Proposal for a Feasible Classification System. *Cryst. Growth Des.* **2016**, *16* (6), 3237−3243.
(17) Akhtaruzzaman; Khan, S.; Dutta, B.; Kannan, T. S.; Kumar Kole, G.; Hedayetullah Mir, M. Cocrystals for Photochemical Solid-State Reactions: An Account on Crystal Engineering Perspective. *Coord. Chem. Rev.* **2023**, *483*, 215095.
(18) MacGillivray, L. R.; Reid, J. L.; Ripmeester, J. A. Supramolecular Control of Reactivity in the Solid State Using Linear Molecular Templates. *J. Am. Chem. Soc.* **2000**, *122*, 7817−7818.
(19) Friščić, T.; Elacqua, E.; Dutta, S.; Oburn, S. M.; MacGillivray, L. R. Total Syntheses Supramolecular Style: Solid-State Construction of [2.2]Cyclophanes with Modular Control of Stereochemistry. *Cryst. Growth Des.* **2020**, *20* (4), 2584−2589.
(20) MacGillivray, L. R. Organic Synthesis in the Solid State via Hydrogen-Bond-Driven Self-Assembly. *J. Org. Chem.* **2008**, *73*, 3311−3317.
(21) Gao, X.; Friščić, T.; MacGillivray, L. R. Supramolecular Construction of Molecular Ladders in the Solid State. *Angew. Chem.* **2004**, *116* (2), 234−238.
(22) Macgillivray, L. R.; Papaefstathiou, G. S.; Friščić, T.; Hamilton, T. D.; Bučar, D. K.; Chu, Q. R.; Varshney, D. B.; Georgiev, I. G. Supramolecular Control of Reactivity in the Solid State: From Templates to Ladderanes to Metal-Organic Frameworks. *Acc. Chem. Res.* **2008**, *41* (2), 280−291.
(23) Friščić, T.; MacGillivray, L. R. Reversing the Code of a Template-Directed Solid-State Synthesis: A Bipyridine Template That Directs a Single-Crystal-to-Single-Crystal [2 + 2] Photodimerisation of a Dicarboxylic Acid. *Chem. Commun.* **2005**, No. 46, 5748−5750.
(24) Ito, Y.; Kitada, T.; Horiguchi, M. Coerced Photodimerization Reaction in the Solid State through Amine Salt Formation. *Tetrahedron* **2003**, *59* (37), 7323−7329.
(25) Michaelides, A.; Skoulika, S.; Siskos, M. G. Assembly of a Photoreactive Coordination Polymer Containing Rectangular Grids. *Chem. Commun.* **2004**, *2004* (21), 2418−2419.
(26) Campillo-Alvarado, G.; Brannan, A. D.; Swenson, D. C.; MacGillivray, L. R. Exploiting the Hydrogen-Bonding Capacity of Organoboronic Acids to Direct Covalent Bond Formation in the Solid State: Templation and Catalysis of the [2 + 2] Photodimerization. *Org. Lett.* **2018**, *20* (17), 5490−5492.
(27) Caronna, T.; Liantonio, R.; Logothetis, T. A.; Metrangolo, P.; Pilati, T.; Resnati, G. Halogen Bonding and Π···π Stacking Control Reactivity in the Solid State. *J. Am. Chem. Soc.* **2004**, *126* (14), 4500−4501.
(28) Sinnwell, M. A.; MacGillivray, L. R. Halogen-Bond-Templated [2 + 2] Photodimerization in the Solid State: Directed Synthesis and Rare Self-Inclusion of a Halogenated Product. *Angew. Chem., Int. Ed.* **2016**, *55* (10), 3477−3480.
(29) Quentin, J.; C Swenson, D.; R MacGillivray, L. Supramolecular Sandwiches: Halogen-Bonded Coformers Direct [2 + 2] Photoreactivity in Two-Component Cocrystals. *Molecules* **2020**, *25* (4), 907.
(30) De Santis, A.; Forni, A.; Liantonio, R.; Metrangolo, P.; Pilati, T.; Resnati, G. N···Br Halogen Bonding: One-Dimensional Infinite Chains through the Self-Assembly of Dibromotetrafluorobenzenes with Dipyridyl Derivatives. *Chem.—Eur. J.* **2003**, *9* (16), 3974−3983.
(31) Sinnwell, M. A.; Blad, J. N.; Thomas, L. R.; MacGillivray, L. R. Structural Flexibility of Halogen Bonds Showed in a Single-Crystal-to-Single-Crystal [2 + 2] Photodimerization. *IUCrJ.* **2018**, *5*, 491−496.
(32) Campillo-Alvarado, G.; D'mello, K. P.; Swenson, D. C.; Santhana Mariappan, S. V.; Höpfl, H.; Morales-Rojas, H.; MacGillivray, L. R. Exploiting Boron Coordination: B←N Bond Supports a [2 + 2] Photodimerization in the Solid State and Generation of a Diboron Bis-Tweezer for Benzene/Thiophene Separation. *Angew. Chem., Int. Ed.* **2019**, *58* (16), 5413−5416.
(33) Campillo-Alvarado, G.; Li, C.; Feng, Z.; Hutchins, K. M.; Swenson, D. C.; Höpfl, H.; Morales-Rojas, H.; Macgillivray, L. R. Single-Crystal-to-Single-Crystal [2 + 2] Photodimerization Involving B←N Coordination with Generation of a Thiophene Host. *Organometallics* **2020**, *39* (12), 2197−2201.
(34) Jon, S. Y.; Ko, Y. H.; Park, S. H.; Kim, H. J.; Kim, K. A Facile, Stereoselective [2 + 2] Photoreaction Mediated by Cucurbit[8]Uril. *Chem. Commun.* **2001**, *1* (19), 1938−1939.
(35) D'Agostino, S.; Boanini, E.; Braga, D.; Grepioni, F. Size Matters: [2 + 2] Photoreactivity in Macro- and Microcrystalline Salts of 4-Aminocinnamic Acid. *Cryst. Growth Des.* **2018**, *18* (4), 2510−2517.
(36) Ito, Y.; Borecka, B.; Trotter, J.; Scheffer, J. R. Control of Solid-State Photodimerization of Trans-Cinnamic Acid by Double Salt Formation with Diamines. *Tetrahedron Lett.* **1995**, *36* (34), 6083−6086.
(37) Yagci, B. B.; Zorlu, Y.; Türkmen, Y. E. Template-Directed Photochemical Homodimerization and Heterodimerization Reactions of Cinnamic Acids. *J. Org. Chem.* **2021**, *86* (18), 13118−13128.
(38) Zitt, H.; Dix, I.; Hopf, H.; Jones, P. G. 4,15-Diamino[2.2]-Paracyclophane, a Reusable Template for Topochemical Reaction Control in Solution. *Eur. J. Org Chem.* **2002**, *2002* (14), 2298−2307.
(39) König, B.; Leue, S.; Horn, C.; Caudan, A.; Desvergne, J.-P.; Bouas-Laurent, H. Synthesis of Medium-Size Macrocycles by Cinnamate [2 + 2] Photoaddition. *Liebigs Ann.* **1996**, *1996* (8), 1231−1233.
(40) Ghosn, M. W.; Wolf, C. Stereocontrolled Photodimerization with Congested 1,8-Bis(4′-Anilino) Naphthalene Templates. *J. Org. Chem.* **2010**, *75* (19), 6653−6659.
(41) *CrysAlisPro*, Version 1.171.37.35; Rigaku Oxford Diffraction, 2014.
(42) Sheldrick, G. M. SHELXT - Integrated Space-Group and Crystal-Structure Determination. *Acta Crystallogr.* **2015**, *71*, 3−8.

https://doi.org/10.1021/acs.cgd.3c01449
Cryst. Growth Des. 2024, 24, 2117−2125

(43) Sheldrick, G. M. Crystal Structure Refinement with SHELXL. *Acta Crystallogr.* **2015**, *71*, 3−8.
(44) Spek, A. L. Structure Validation in Chemical Crystallography. *Acta Crystallogr.* **2009**, *65*, 148−155.
(45) MacRae, C. F.; Sovago, I.; Cottrell, S. J.; Galek, P. T. A.; McCabe, P.; Pidcock, E.; Platings, M.; Shields, G. P.; Stevens, J. S.; Towler, M.; Wood, P. A. Mercury 4.0: From Visualization to Analysis, Design and Prediction. *J. Appl. Crystallogr.* **2020**, *53*, 226−235.
(46) ChemSpider. 4,6-Dichlororesorcinol. https://www.chemspider.com/Chemical-Structure.60631.html (accessed Jan 05, 2024).
(47) Bradley, J.-C.; Abraham, M. H.; Acree, W. E.; Lang, A. S. I. D.; Beck, S. N.; Bulger, D. A.; Clark, E. A.; Condron, L. N.; Costa, S. T.; Curtin, E. M.; Kurtu, S. B.; Mangir, M. I.; McBride, M. J. Determination of Abraham Model Solute Descriptors for the Monomeric and Dimeric Forms of Trans-Cinnamic Acid Using Measured Solubilities from the Open Notebook Science Challenge. *Chem. Cent. J.* **2015**, *9* (1), 11.
(48) Lorenzo, D. A.; Forrest, S. J. K.; Sparkes, H. A. Crystal Engineering: Co-Crystals of Cinnamic Acid Derivatives with a Pyridyl Derivative Co-Crystallizer. *Acta Crystallogr., Sect. B: Struct. Sci., Cryst. Eng. Mater.* **2016**, *72* (1), 87−95.

https://doi.org/10.1021/acs.cgd.3c01449
Cryst. Growth Des. 2024, 24, 2117−2125